

Efficient Topology Design Algorithms for Power Grid Stability

Siddharth Bhela, Harsha Nagarajan, Deepjyoti Deka, and Vassilis Kekatos

Abstract—The dynamic response of power grids to small disturbances influences their overall stability. This paper examines the effect of topology on the linear time-invariant dynamics of electricity networks. The proposed framework utilizes \mathcal{H}_2 -norm based stability metrics to study the optimal selection of transmission lines on existing networks as well as the topology design of new networks. The design task is first posed as an NP-hard mixed-integer nonlinear program (MINLP) that is exactly reformulated as a mixed-integer linear program (MILP) using McCormick linearization. To improve computation time, a cutting plane generation procedure is put forth that is able to interject the MILP solver and augment additional constraints to the problem on-the-fly. Moreover, graph-theoretic properties are exploited to derive valid inequalities (cuts) and tighten bounds on the continuous optimization variables to significantly accelerate the solver run times. The efficacy of our approach in designing optimal grid topologies is demonstrated through numerical tests on the IEEE 39-bus network.

I. INTRODUCTION

Widespread adoption of new grid technologies is continuously changing the face of our modern electricity networks. Increased penetration of renewable energy sources and changing load patterns has lead to higher volatility in power networks [1]. The stochastic nature of renewables and active loads is likely to produce recurring disturbances that will require careful planning and design of power networks with stability in mind [1]. Additionally, the loss of rotational inertia in systems with high percentage of renewables will significantly reduce the capability of power grids to handle such disturbances [2].

While several works have explored the placement of virtual inertia to improve the dynamic performance of power networks, it is not well understood how grid topology affects transient stability. Utilities currently run detailed and time-consuming dynamic simulations to deduce how a change in network topology would impact the overall grid stability. Recent works have shown that the grid Laplacian matrix eigenvalues allows us to quantify the effect of grid topology on the power network [3]. Our work is further motivated by the claim that grid robustness against low frequency disturbances is determined by the connectivity of the network [3]. Past studies have looked at designing grid topologies for specific goals such as reduction of transient line losses [1], improvement in feedback control [4], and coherence-based network design [5].

This paper investigates the effect of topology on power system dynamics. For a variety of \mathcal{H}_2 -norm based stability metrics, such as reduction of line losses, fast damping of oscillations, and network synchronization, our previous works [6], [7] presented methods that can be used to optimally design power grid topologies. In [7], we presented

reformulations of the combinatorial topology design task that allowed us to solve the problem to optimality, albeit with forbiddingly slow run times. Moreover, the focus in [7] was primarily on the design of radial networks and optimal placement of new lines on existing networks. In this work, we focus on developing efficient algorithms for designing both radial and loopy networks. These improvements are the result of the following key contributions: *i*) Tight SDP (semi-definite programming) formulations and a valid eigenvector-based sparse cut-generation procedure that significantly improves the solving time for the topology design task (see Section III); *ii*) Valid cuts based on graph-theoretic properties and tighter bounds on the continuous optimization variables that accelerate solver run times for larger scale problems (see Section IV); *iii*) A new bound tightening technique that can provide valid bounds for the design of meshed networks (see Section IV); and *iv*) New conditions for supermodularity of the topology design problem (see Section V).

Notation: Column vectors are denoted by lower case letters; matrices by upper case letters; and sets by calligraphic symbols. The cardinality of set \mathcal{X} is denoted by $|\mathcal{X}|$ and \emptyset is an empty set. Given a real-valued sequence $\{x_1, \dots, x_N\}$, x is the $N \times 1$ vector obtained by stacking the entries x_i and $\text{dg}(\{x_i\})$ is the corresponding diagonal matrix. The operator $(\cdot)^\top$ stands for transposition. The $N \times N$ identity matrix is represented by I_N . The canonical vector e_i has a 1 at the i -th entry and is 0 elsewhere. The time derivative of θ is denoted by $\dot{\theta} := \frac{d\theta}{dt}$. $M \succeq 0$ implies that M is a positive semi-definite matrix.

II. GRID MODELING AND STABILITY METRICS

An electric power network with $N+1$ nodes can be represented by a graph $\mathcal{G} = (\mathcal{V}, \mathcal{E})$, where $\mathcal{V} := \{1, 2, \dots, N+1\}$ corresponds to nodes and edges in \mathcal{E} correspond to undirected lines. Let node $i = 1$ be the reference, and collect the remaining nodes in set $\mathcal{V}_r := \mathcal{V} \setminus \{1\}$. The susceptance of line $(i, j) \in \mathcal{E}$ connecting nodes i and $j \in \mathcal{V}$ is denoted by $b_{ij} > 0$. Then, L represents the $(N+1) \times (N+1)$ susceptance Laplacian matrix of the graph \mathcal{G} and is defined as

$$L_{ij} := \begin{cases} \sum_{(i,j) \in \mathcal{E}} b_{ij} & , \text{ if } i = j \\ -b_{ij} & , \text{ if } (i, j) \in \mathcal{E} \\ 0 & , \text{ otherwise.} \end{cases}$$

We consider a small-signal disturbance setup and eliminate non-dynamic load nodes using Kron reduction [8]. Each node $i \in \mathcal{V}$ is associated with a generator's rotor angle θ_i , frequency $\omega_i = \dot{\theta}_i$, inertia constant M_i , and damping coefficient D_i ; see [8]. If a node i hosts an ensemble

of devices, the parameters M_i and D_i represent lumped characterizations of the collective behavior of the hosted devices [9]. Without loss of generality, the quantities (θ_i, ω_i) will henceforth refer to deviations of nodal phase angles and frequencies from their steady-state values. Using these definitions, the state-space representation of the linearized power grid dynamics can be expressed as [8]

$$\begin{bmatrix} \dot{\theta} \\ \dot{\omega} \end{bmatrix} = \underbrace{\begin{bmatrix} 0 & I_N \\ -M^{-1}L & -M^{-1}D \end{bmatrix}}_{A:=} \begin{bmatrix} \theta \\ \omega \end{bmatrix} + \underbrace{\begin{bmatrix} 0 \\ M^{-1} \end{bmatrix}}_{B:=} u \quad (1)$$

where $M := \text{dg}(\{M_i\})$ and $D := \text{dg}(\{D_i\})$ are the $(N+1) \times (N+1)$ matrices collecting the inertia and damping constants across all nodes; the $(N+1)$ -long vectors θ , ω , and u stack respectively the phase angles, frequencies, and power disturbances at each node. The subsequent analysis relies on the ensuing assumption, which has been justified in several existing works [1], [7], [10].

Assumption 1. *The constants (M_i, D_i) are positive and $D_i = c$ for all $i \in \mathcal{V}$ (identical damping).*

Given the state-space model in (1), our goal is to design power network topologies that minimize the expected steady-state value of a generalized control objective combining angle deviations and frequency excursions [6], [9]

$$f(t) := \sum_{i \in \mathcal{V}} \left[\sum_{j \neq i} w_{ij} (\theta_i(t) - \theta_j(t))^2 + s_i \omega_i^2(t) \right] \quad (2)$$

for given non-negative weights $\{w_{ij}\}$ and $\{s_i\}$. The weights w_{ij} induce a connected weighted graph \mathcal{G}_w that may be different from \mathcal{G} . Let W be the Laplacian matrix of graph \mathcal{G}_w and define $S := \text{dg}(\{s_i\})$. Then, it is easy to see that $f(t) = \|y(t)\|_2^2$, where

$$y(t) := \underbrace{\begin{bmatrix} W^{1/2} & 0 \\ 0 & S^{1/2} \end{bmatrix}}_{C:=} \begin{bmatrix} \theta(t) \\ \omega(t) \end{bmatrix}. \quad (3)$$

The importance of the generalized control objective in (2) is that by varying (W, S) , one can capture different stability metrics and study them under a unified framework [6]. Note that the network coherence metric considered in the numerical tests corresponds to the case of $S = 0$ [6] and

$$W = I_{N+1} - \frac{1}{N+1} \mathbf{1}_{N+1} \mathbf{1}_{N+1}^\top$$

The expected steady-state value of $f(t)$ can be interpreted as the squared \mathcal{H}_2 -norm of the linear time-invariant (LTI) system described by (1) and (3). This system will be compactly denoted by $H := (A, B, C)$. Leveraging this link, the generalized control objective can be expressed as

$$\|H\|_{\mathcal{H}_2}^2 = \text{Tr}(B^\top Q B) \quad (4)$$

where $Q \succeq 0$ is the observability Gramian matrix of the LTI system H , and can be computed as the solution to the Lyapunov equation [11, Ch. 5]

$$A^\top Q + QA = -C^\top C. \quad (5)$$

The ensuing sections select network topologies that minimize the stability objective of (4).

III. OPTIMAL DESIGN OF GRID TOPOLOGIES

Consider a graph $\hat{\mathcal{G}} = (\mathcal{V}, \hat{\mathcal{E}})$, where $\hat{\mathcal{E}}$ is the set of all candidate lines. The goal is to find a subset of lines $\mathcal{E} \subseteq \hat{\mathcal{E}}$, so that the resultant power network minimizes the stability objective in (4). Because adding lines can be costly and utilities have limited budgets, we further impose the constraint that $|\mathcal{E}| \leq K$ with $K \geq N$. By setting $K = N$, a radial topology can be enforced. The topology design task can be now posed as [7]

$$\arg \min_{\mathcal{E} \in \hat{\mathcal{E}}} \text{Tr}(B^\top Q B) \quad (6a)$$

$$\text{s.to } |\mathcal{E}| \leq K \quad (6b)$$

$$A^\top Q + QA = -C^\top C \quad (6c)$$

$$\text{graph } \mathcal{E} \text{ is connected.} \quad (6d)$$

Under Assumption 1 and by solving for Q from (6c), the objective of (6) can be shown to be proportional to $\text{Tr}(WL^+) + \text{Tr}(SM^{-1})$; see [9], [6], [1]. The term $\text{Tr}(SM^{-1})$ does not depend on the grid topology and can be ignored. Problem (6) can be then rewritten as [7]

$$\arg \min_{\mathcal{E} \in \hat{\mathcal{E}}} \text{Tr}(WL^+) \quad (7)$$

$$\text{s.to } |\mathcal{E}| \leq K, \quad \text{rank}(L) = N$$

where the rank constraint ensures that the resultant graph is connected. The objective in (7) can be written in terms of the inverse of the *reduced Laplacian* matrix of $\hat{\mathcal{G}}$ [7].

Lemma 1. *If \tilde{W} and \tilde{L} are the $N \times N$ matrices obtained after removing the first row and column from W and L , respectively, then $\text{Tr}(WL^+) = \text{Tr}(\tilde{W}\tilde{L}^{-1})$.*

To express the optimization in (7) over $\hat{\mathcal{E}}$ in a more convenient form, let us associate each line $\ell \in \hat{\mathcal{E}}$ with a binary variable z_ℓ , which is $z_\ell = 1$ if line ℓ is selected (that is $\ell \in \mathcal{E}$); and $z_\ell = 0$, otherwise. If we collect variables $\{z_\ell\}_{\ell \in \hat{\mathcal{E}}}$ in vector z , then z must lie in the set

$$\mathcal{Z} := \left\{ z : z^\top \mathbf{1}_{|\hat{\mathcal{E}}|} \leq K, z \in \{0, 1\}^{|\hat{\mathcal{E}}|} \right\}. \quad (8)$$

Based on the line selection vector z , the reduced susceptibility Laplacian of $\hat{\mathcal{G}}$ can be expressed as

$$\tilde{L}(z) = \sum_{(i,j) \in \hat{\mathcal{E}}} z_{ij} b_{ij} a_{ij} a_{ij}^\top. \quad (9)$$

Here, each vector a_{ij} corresponds to line $(i, j) \in \hat{\mathcal{E}}$. Its n -th entry $[a_{ij}]_n$ is $+1$, if $n = i$; -1 , if $n = j$; and 0 otherwise. Given the explicit form of $\tilde{L}(z)$, it is not hard to see that the objective in (7) is a monotone function that is minimized when all lines in $\hat{\mathcal{E}}$ are selected. Utilizing Lemma 1 together with (9), the optimization in (7) can be equivalently written as an MINLP [7]

$$(X^*, z^*) \in \arg \min_{X, z \in \mathcal{Z}} \text{Tr}(\tilde{W}X) \quad (10a)$$

$$\text{s.to } \tilde{L}(z)X = I_N. \quad (10b)$$

Constraint (10b) enforces $X = \tilde{L}^{-1}(z)$, and thus, matrix $\tilde{L}(z)$ to be full-rank at optimality. Problem (10) is non-convex due to the binary nature of z and the bilinear constraints in (10b). To handle the latter, we adopt McCormick linearization [12], which is briefly reviewed next.

Constraint (10b) involves bilinear terms $z_\ell X_{ij}$ for all $\ell \in \hat{\mathcal{E}}$ and $i, j \in \mathcal{V}_r$. For every term, introduce an auxiliary variable

$$y_{\ell ij} = z_\ell X_{ij} \quad (11)$$

and let the entries X_{ij} lie within bounds $[\underline{X}_{ij}, \bar{X}_{ij}]$. Since z_ℓ is binary, the following inequalities hold true

$$y_{\ell ij} \geq z_\ell \underline{X}_{ij}, \quad y_{\ell ij} \geq X_{ij} + z_\ell \bar{X}_{ij} - \bar{X}_{ij} \quad (12a)$$

$$y_{\ell ij} \leq z_\ell \bar{X}_{ij}, \quad y_{\ell ij} \leq X_{ij} + z_\ell \underline{X}_{ij} - \underline{X}_{ij}. \quad (12b)$$

One can replace the bilinear terms in (10b) by $y_{\ell ij}$'s, drop equation (11), and enforce (12) as additional constraints for all $\ell \in \hat{\mathcal{E}}$ and $i, j \in \mathcal{V}_r$ to get an MILP reformulation of (10). It is not hard to show that this reformulation is *exact*, i.e., $y_{\ell ij} = z_\ell X_{ij}$ because z is binary.

Through the aforementioned process, problem (10) is reformulated to an MILP over variables $\{X_{ij}\}$, $\{z_\ell\}$, and $\{y_{\ell ij}\}$, and can thus be handled by modern MILP solvers such as Gurobi or CPLEX. Nonetheless, MILPs with McCormick linearization can be forbiddingly complex to solve if the bounds $(\underline{X}_{ij}, \bar{X}_{ij})$ on each X_{ij} are arbitrarily wide. To address this issue, we first explain how additional valid cuts can be included to strengthen the MILP formulation. Consider the constraint

$$Y \succeq 0, \quad \text{where } Y = \begin{bmatrix} X & I_N \\ I_N & \tilde{L}(z) \end{bmatrix} \quad (13)$$

that is clearly valid for (10). One could replace (10b) with (13), but that would require solving a much harder mixed-integer semi-definite program (MISDP). Instead, we observe that the SDP constraint in (13) could strengthen the bounds in MILP solvers and reduce the size of the branch-and-bound tree. However, since enforcing such constraints is non-trivial, one can exploit the alternative characterization of an SDP matrix by selecting S vectors, $v_s \in \mathbb{R}^N$, and augment the MILP in (10) with the linear cuts

$$v_s^\top Y v_s \geq 0, \quad s = 1, \dots, S. \quad (14)$$

Vectors $\{v_s\}_{s=1}^S$ could be random, e.g., independently drawn as $v_s \sim \mathcal{N}(0, \mathbf{I}_N)$. However, it is known that adding such constraints may not tighten the MILP formulation [13]. We will explore how v_s can be chosen judiciously to yield more meaningful cuts.

2k-sparse eigenvector cuts: Let (z^r, X^r) be the solution to the MILP formulation of (10) obtained by relaxing $z \in \{0, 1\}^{|\hat{\mathcal{E}}|}$ to the box constraints $z \in [0, 1]^{|\hat{\mathcal{E}}|}$. Moreover, let Y^r be the matrix obtained by substituting (z^r, X^r) in Y . Heed that the *relaxed* MILP formulation is not exact, i.e., (z^r, X^r) may not satisfy constraint (10b). In fact, (z^r, X^r) may not satisfy constraint (13) either. A valid cut can be derived from the latter observation, as explained next.

Another way of enforcing (13) is to ensure that all the eigenvalues of Y are non-negative. This can be accomplished

by assigning v_s in (14) to be the eigenvectors corresponding to the negative eigenvalues of Y^r . Notice that the cuts in (14) do not have to be added only once at the beginning of the solution process (root node), but can also be added by interjecting the MILP solver at every branch-and-bound node when a new relaxed solution is found for (10). However, since the eigenvectors $\{v_s\}$ are generally non-sparse, each one of the linear inequality constraints $v_s^\top Y v_s$ will couple almost all entries in Y , that is roughly N^2 variables. Such dense constraints can be often detrimental to the solver's overall solution time. To alleviate this, we include cuts stemming from a sparse v_s . To this end, let us partition $v_s^\top := [v_{s_1}^\top \ v_{s_2}^\top]$ such that

$$v_s^\top Y v_s = v_{s_1}^\top \tilde{L} v_{s_1} + v_{s_2}^\top X v_{s_2} + 2v_{s_1}^\top v_{s_2}. \quad (15)$$

Since constraint (13) is equivalent to $X \succeq 0$ and $X \succeq \tilde{L}^{-1}(z)$; see [14, Sec. A.5.5], the first two entries in the summand of (15) are non-negative and only the last term

$$2v_{s_1}^\top v_{s_2} = 2 \sum_{n=1}^N v_{s_1, n} v_{s_2, n} \quad (16)$$

contributes to $v_s^\top Y v_s$ being negative. Keeping this in mind, the idea here is to identify the k most negative entries out of the N summands in (16). For the related indices n , we maintain the entries of (v_{s_1}, v_{s_2}) , whereas for the remaining indices we set the corresponding entries to zero. Thus, the modified vectors (v_{s_1}, v_{s_2}) are k -sparse and bear the same sparsity pattern. Vector v_s is then $2k$ -sparse.

While the $2k$ -sparse cuts can effectively enforce constraint (13) in the MILP formulation, there is a trade-off between the number of such cuts and improvement in solution time. Recall that because the cuts in (14) are added to the solution process on-the-fly, adding too many cuts can significantly slow down the solver. To circumvent this, we suggest adding only those vectors v_s that correspond to the negative eigenvalues of Y^r falling below a pre-defined threshold γ and/or limit the total number of constraints added.

So far, we presented a procedure to generate eigenvector-based valid cuts which strengthened the relaxation of the MILP. We next pursue tighter, non-trivial bounds $(\underline{X}_{ij}, \bar{X}_{ij})$ on the entries of X to further tighten the McCormick linearizations in (12) and expedite solving times of (10).

IV. VALID INEQUALITIES FOR BOUND TIGHTENING

Exploiting various graph-theoretic properties, different bounds can be derived on X_{ij} 's. This section considers two classes of topology design tasks: *i*) augmenting an existing connected network by additional lines; *ii*) designing a new network topology afresh. The former task can also be viewed as a topology switching problem.

A. Augmenting Existing Power Networks

This problem setup considers an existing network described by $\mathcal{G}_e = (\mathcal{V}, \mathcal{E}_e)$ where the goal is to select additional lines from $\hat{\mathcal{E}} \setminus \mathcal{E}_e$ to improve stability. In essence, this corresponds to the problem in (10) with the entries of z

associated with the lines in \mathcal{E}_e being set to one. Based on (9), the reduced Laplacian matrices of the existing network \mathcal{G}_e and the full network $\hat{\mathcal{G}}$ are $\tilde{L}_e := \sum_{(i,j) \in \mathcal{E}_e} b_{ij} a_{ij} a_{ij}^\top$ and $\tilde{L}_f := \sum_{(i,j) \in \hat{\mathcal{E}}} b_{ij} a_{ij} a_{ij}^\top$, respectively.

Under this setup and assuming that \mathcal{G}_e is connected, the entries of X minimizing (10) under the additional constraints $z_\ell = 1$ for all $\ell \in \mathcal{E}_e$, can be bounded as follows.

Lemma 2. *Given that $\tilde{L}_f^{-1} \preceq X \preceq \tilde{L}_e^{-1}$, the diagonal entries of X are bounded by*

$$[\tilde{L}_f^{-1}]_{ii} \leq X_{ii} \leq [\tilde{L}_e^{-1}]_{ii}, \quad \forall i \in \mathcal{V}_r, \quad (17)$$

and its off-diagonal entries are bounded by

$$\begin{aligned} X_{ij} &\leq [\tilde{L}_f^{-1}]_{ij} + \sqrt{([\tilde{L}_e^{-1}]_{jj} - [\tilde{L}_f^{-1}]_{jj})([\tilde{L}_e^{-1}]_{ii} - [\tilde{L}_f^{-1}]_{ii})} \\ X_{ij} &\geq [\tilde{L}_e^{-1}]_{ij} - \sqrt{([\tilde{L}_e^{-1}]_{jj} - [\tilde{L}_f^{-1}]_{jj})([\tilde{L}_e^{-1}]_{ii} - [\tilde{L}_f^{-1}]_{ii})} \end{aligned}$$

for all $i, j \in \mathcal{V}_r$ with $j \neq i$.

Proof. Since $X \succeq \tilde{L}_f^{-1}$, it follows that for all v

$$v^\top (X - \tilde{L}_f^{-1})v \geq 0. \quad (19)$$

Selecting $v = e_i - \delta e_j$ for some $\delta \geq 0$ in (19) yields

$$X_{ii} + \delta^2 X_{jj} - 2\delta X_{ij} \geq [\tilde{L}_f^{-1}]_{ii} + \delta^2 [\tilde{L}_f^{-1}]_{jj} - 2\delta [\tilde{L}_f^{-1}]_{ij}. \quad (20)$$

Setting $\delta = 0$ provides the LHS of (17). The RHS of (17) can be obtained by exploiting $\tilde{L}_e^{-1} \succeq X$ likewise.

For the off-diagonal entries of X , rearrange (20) if $\delta > 0$ and substitute X_{ii} and X_{jj} with the respective upper bounds from (17) to obtain

$$X_{ij} \leq [\tilde{L}_f^{-1}]_{ij} + \frac{[\tilde{L}_e^{-1}]_{ii} - [\tilde{L}_f^{-1}]_{ii}}{2\delta} + \delta \frac{[\tilde{L}_e^{-1}]_{jj} - [\tilde{L}_f^{-1}]_{jj}}{2}.$$

The RHS of the upper bound on X_{ij} can be minimized over $\delta > 0$ to obtain

$$\delta^* := \sqrt{\frac{[\tilde{L}_e^{-1}]_{ii} - [\tilde{L}_f^{-1}]_{ii}}{[\tilde{L}_e^{-1}]_{jj} - [\tilde{L}_f^{-1}]_{jj}}}.$$

Plugging δ^* back into the bounds completes the proof. The lower bound on X_{ij} can be obtained by exploiting the fact that $\tilde{L}_e^{-1} \succeq X$ similarly. \blacksquare

To provide some alternate bounds on the entries of X , let us consider the following inequality

$$X_{ii} + X_{jj} - 2X_{ij} \leq d_{ij} + \epsilon \quad \forall i, j \in \mathcal{V}_r \quad (21)$$

where the LHS of (21) is equivalent to the effective resistance R_{ij} of the graph; scalar d_{ij} is the distance of the shortest weighted path between nodes i and j on \mathcal{G}_e ; and ϵ is an arbitrarily small positive number [15]. The shortest path between all pairs $(i, j) \in \mathcal{V}_r$ can be obtained using the Floyd-Warshall algorithm [16]. Note that for the special case where there is a unique path between nodes i and j , the bound in (21) is tight, that is, $R_{ij} = d_{ij}$. Moreover, the effective resistance R_{ij} does not increase when edges are added [15]. This simple fact can be exploited to obtain the following bounds.

Lemma 3. *The off-diagonal entries of X are lower bounded by*

$$\frac{[\tilde{L}_f^{-1}]_{ii} + [\tilde{L}_f^{-1}]_{jj} - d_{ij} - \epsilon}{2} \leq X_{ij} \quad \forall i, j \in \mathcal{V}_r \quad (22)$$

Proof. The bound can be simply obtained by rearranging the terms in (21) and substituting the lower bounds for the diagonal entries (X_{ii}, X_{jj}) from (17). \blacksquare

Once all valid bounds are found for entries in X , only the tightest bounds are retained to accelerate the performance of the solver. Note that the reduced Laplacian matrix \tilde{L}_e of the existing network \mathcal{G}_e is invertible only if \mathcal{G}_e is connected. If not, one could obtain bounds on X_{ij} 's by imposing a meshed or radial structure on the sought topology as discussed next.

B. Designing New Power Networks

The setup considered here designs a network afresh. Bounds for design of radial network topologies were considered in our previous work [7]. Here we focus on presenting a novel approach to derive bounds on the entries of X for meshed networks. To this end, note that the lower bound in (17) is also valid for the design of new networks. Because X is an inverse M-matrix, the off-diagonal entries can be lower bounded as $X_{ij} \geq 0$, for all $i, j \in \mathcal{V}_r, i \neq j$ [17].

Exploiting the structure of $\hat{\mathcal{G}} = (\mathcal{V}, \hat{\mathcal{E}})$, we can provide additional information on the entries of X to accelerate (10) for designing radial and meshed grids alike. For example, if $\hat{\mathcal{G}}$ is disconnected upon removing edge $\ell \in \hat{\mathcal{E}}$, then ℓ belongs to the sought network topology and $z_\ell^* = 1$ before solving (10). Such critical edges $\mathcal{E}_c \subset \hat{\mathcal{E}}$ can be identified using the algorithm presented in our previous work [7] and the entries of z corresponding to these edges can be safely set to 1. This process not only reduces the binary search for z^* in (10), but it further tightens the lower bounds on certain X_{ij} 's.

Corollary 1. *Suppose a critical edge $\ell = (i, j) \in \hat{\mathcal{E}}$ partitions the nodes of $\hat{\mathcal{G}}$ into two disjoint connected components \mathcal{V}_ℓ and its complement $\bar{\mathcal{V}}_\ell$. If \mathcal{V}_ℓ contains nodes $(i, 1)$ and $\bar{\mathcal{V}}_\ell$ contains node j , then we can tighten the lower bound*

$$\frac{[\tilde{L}_f^{-1}]_{ii} + [\tilde{L}_f^{-1}]_{jj} - \hat{d}_{ij} - \epsilon}{2} \leq X_{ij} \quad (23)$$

where \hat{d}_{ij} is the shortest path (susceptance of edge ℓ) between nodes i and j on graph $\hat{\mathcal{G}}$. Similarly, for the design of radial networks one can tighten the lower bounds as

$$\hat{d}_{i1} - \epsilon \leq X_{ij} \quad (24)$$

Proof. Because edge ℓ is the only connection between nodes i and j on graph $\hat{\mathcal{G}}$, this edge is also the shortest path between the two nodes and must belong to the sought network topology. The bound in (23) can then be shown to be valid using the arguments in the proof for Lemma 3. To obtain the bound in (24), we refer the readers to arguments presented in our previous work [7, Lemma 4]. \blacksquare

So far we have obtained analytical lower bounds on the entries of X , that is $\underline{X} \leq X$ for the known matrix \underline{X} .

Using these lower bounds, valid upper bounds on entries of symmetric matrix X can be found by solving $\frac{N(N+1)}{2}$ linear programs of the form

$$\max_X \alpha^\top X \beta \quad (25a)$$

$$\text{s. to } \text{Tr}(\tilde{W}X) \geq \text{Tr}(\tilde{W}X^r), \quad (25b)$$

$$\text{Tr}(\tilde{W}X) \leq \text{Tr}(\tilde{W}X^f), \quad (25c)$$

$$X_{ii} + X_{jj} - 2X_{ij} \geq [\tilde{L}_f^{-1}]_{ii} + [\tilde{L}_f^{-1}]_{jj} - 2[\tilde{L}_f^{-1}]_{ij} \quad (25d)$$

$$X_{ii} + X_{jj} - 2X_{ij} \leq \hat{d}_{ij} + \epsilon \quad \forall (i, j) \in \mathcal{E}_c \quad (25e)$$

$$X_{ii} \geq X_{ij} \quad \forall i, j \in \mathcal{V}_r, i \neq j \quad (25f)$$

$$X \leq X \quad (25g)$$

where the vectors (α, β) in the cost can be set as

1) $\alpha = \beta = e_i$ to upper bound X_{ii} .

2) $\alpha = e_i$ and $\beta = e_j$ to upper bound X_{ij} .

Matrix X^f is any feasible solution to (10), constraint (25d) can be shown to be valid by simply substituting $\delta = 1$ in (20), the cut in (25e) is derived using (21) and Corollary 1, and the inequality in (25f) is a property of inverse M-matrices [17]. The bound in (25g) is understood entry-wise.

Beyond tightening the bounds on the entries of X and adding constraints of the form in (14), constraints (25e)–(25f) are also appended to the MILP formulation of (10) to improve computational efficiency. We henceforth refer to this as the *tightened* MILP formulation.

Remark 1. Our previous work in [7] relied on the limiting assumption that there exists a node in \mathcal{V} that is incident to exactly one edge in $\hat{\mathcal{E}}$. By fixing this node to be the reference node we were able to obtain several graph-theoretic bounds that are valid for the design of radial networks. If no such node exists or the chosen reference node has multiple connections, then one can utilize the approach in (25) to find looser yet valid bounds on the entries of X .

Remark 2. For the special case where removing all connections to the reference node results in more than two connected components, matrix X becomes block diagonal in structure and each sub-network (meshed or radial) can be designed independently by solving a separate MILP. In that sense, the problem in (10) is parallelizable.

While the focus so far has been on developing techniques to exactly solve the topology design problem, we next explore conditions under which a greedy scheme would perform well.

V. SUPERMODULARITY OF EDGE AUGMENTATION

For a given finite set \mathcal{S} , a function $f : 2^{\mathcal{S}} \rightarrow \mathbb{R}$ is said to be supermodular if for all subsets $\mathcal{A} \subseteq \mathcal{B} \subseteq \mathcal{S}$, and all $\mathcal{C} \in \mathcal{S} \setminus \mathcal{B}$, it holds that [18]

$$f(\mathcal{A} \cup \mathcal{C}) - f(\mathcal{A}) \leq f(\mathcal{B} \cup \mathcal{C}) - f(\mathcal{B})$$

In other words, the returns due to selection of \mathcal{C} are non-diminishing where adding elements to the larger set \mathcal{B} gives larger gains. Minimizing a supermodular decreasing function

is NP-hard. However, it is known that a greedy scheme that iteratively minimizes the objective $f(\mathcal{A} \cup \{s\})$ for $s \in \mathcal{S} \setminus \mathcal{A}$ is at least $1 - 1/e \simeq 63\%$ close to the optimal solution [18].

Lemma 4 ([18]). *Let A^* and A^g be the global and best greedy minimizer to the supermodular decreasing function f , respectively. Then*

$$\frac{f(A^*) - f(A^g)}{f(\emptyset) - f(A^*)} \leq 1/e.$$

In general the edge addition problem is not supermodular and hence strong theoretical guarantees are not permissible. The following theorem lays a restrictive condition under which the set function $f(\hat{\mathcal{E}}) = \text{Tr}(\tilde{W}\tilde{L}^{-1})$ is a supermodular decreasing function of edge addition.

Theorem 2. *The function $\text{Tr}(\tilde{W}\tilde{L}^{-1})$ is decreasing and supermodular in the addition of susceptance weighted edges to set $\mathcal{E}_e \subset \hat{\mathcal{E}}$ if*

$$\begin{aligned} ([\tilde{L}_e^{-1}]_{ik} - [\tilde{L}_e^{-1}]_{il}) - ([\tilde{L}_e^{-1}]_{jk} - [\tilde{L}_e^{-1}]_{jl}) &> 0 \\ ([\tilde{L}_e^{-1}]_{mk} - [\tilde{L}_e^{-1}]_{ml}) - ([\tilde{L}_e^{-1}]_{nk} - [\tilde{L}_e^{-1}]_{nl}) &> 0 \\ ([\tilde{L}_e^{-1}]_{im} - [\tilde{L}_e^{-1}]_{in}) - ([\tilde{L}_e^{-1}]_{jm} - [\tilde{L}_e^{-1}]_{jn}) &> 0 \end{aligned}$$

where (k, l) is an edge in \tilde{W} ($w_{kl} > 0$) while (i, j) and (m, n) are edges added to \tilde{L}_e .

Proof. Let $\mathcal{S} = \{(i, j), (m, n)\}$ such that $\mathcal{S} \notin \mathcal{E}_e$. Define the function $f(\mathcal{E}_e) = \text{Tr}(\tilde{W}\tilde{L}_e^{-1})$ and the positive semi-definite matrix $\Delta = \sum_{r \in \mathcal{S}} b_r a_r a_r^\top$. The Neumann series expansion of $f(\mathcal{E}_e \cup \{\mathcal{S}\})$ is given by

$$\begin{aligned} \text{Tr}(\tilde{W}(\tilde{L}_e + \Delta)^{-1}) &= \text{Tr}(\tilde{W}\tilde{L}_e^{-1}) - \text{Tr}(\tilde{W}\tilde{L}_e^{-1}\Delta\tilde{L}_e^{-1}) + \\ &\quad \text{Tr}(\tilde{W}\tilde{L}_e^{-1}\Delta\tilde{L}_e^{-1}\Delta\tilde{L}_e^{-1}) + \text{higher order terms} \end{aligned}$$

Note that the first-order term is negative for all $b_r \geq 0$ and hence the function is decreasing. To prove that $f(\hat{\mathcal{E}}) = \text{Tr}(\tilde{W}\tilde{L}^{-1})$ is supermodular, we find conditions under which the function is strictly convex. For this, the second derivative of $f(\hat{\mathcal{E}})$ with respect to (b_{ij}, b_{mn}) must be positive

$$\begin{aligned} \frac{\delta^2 f}{\delta b_{ij} \delta b_{mn}} &> 0 \\ \Rightarrow (a_{mn}^\top \tilde{L}_e^{-1} \tilde{W} \tilde{L}_e^{-1} a_{ij})(a_{mn}^\top \tilde{L}_e^{-1} a_{ij}) &> 0 \end{aligned} \quad (27)$$

A sufficient condition for positivity is when both terms on the LHS of (27) are positive. Expanding them we have

$$\begin{aligned} &a_{mn}^\top \tilde{L}_e^{-1} \tilde{W} \tilde{L}_e^{-1} a_{ij} \\ &= \sum_{w_{kl} > 0} w_{kl} \left([\tilde{L}_e^{-1}]_{ik} - [\tilde{L}_e^{-1}]_{il} - [\tilde{L}_e^{-1}]_{jk} + [\tilde{L}_e^{-1}]_{jl} \right. \\ &\quad \left. \left([\tilde{L}_e^{-1}]_{mk} - [\tilde{L}_e^{-1}]_{ml} - [\tilde{L}_e^{-1}]_{nk} + [\tilde{L}_e^{-1}]_{nl} \right) \right) \text{ and} \\ &a_{mn}^\top \tilde{L}_e^{-1} a_{ij} = [\tilde{L}_e^{-1}]_{im} - [\tilde{L}_e^{-1}]_{in} - [\tilde{L}_e^{-1}]_{jm} + [\tilde{L}_e^{-1}]_{jn} \end{aligned}$$

This leads to the conditions for supermodularity. ■

To the best of our knowledge, this is the first time explicit conditions for supermodularity have been provided

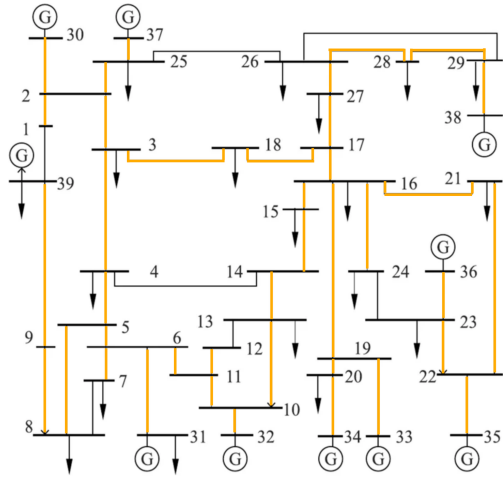


Fig. 1. Optimal meshed (yellow lines) topology with candidate edges from the IEEE 39-bus network (black and yellow lines) [20].

for the topology design problem. Since these conditions are restrictive and do not hold in general, a greedy scheme is unlikely to perform well. This further motivates the need to solve the problem to optimality using our proposed approach in Sections III and IV.

VI. NUMERICAL TESTS

All tests were carried out on a 2.3 GHz Intel Dual-Core i5 laptop with 16GB RAM. The tightened MILP formulation was solved in Julia/JuMP v0.6 [19] using Gurobi v8.1.1. The performance of the tightened MILP formulation was tested for augmenting existing networks as well as for designing new radial and meshed grid topologies. For the augmentation task, the IEEE 39-bus system was used as the pre-existing connected network [20]. The set $\hat{\mathcal{E}}$ consisted of edges in this base network and an additional 22 randomly placed lines. From these lines, we solved (10) for $K = \{5, 6, 7, 8\}$. To satisfy Assumption 1, we assumed $M_i = 10^{-4}$ on all nodes that did not host generators, and $D_i = c = 0.025$ for all $i \in \mathcal{V}$. Additionally, we utilized a threshold value of $\gamma = -0.7$ to limit the total number of eigenvector-based cuts added to the problem on-the-fly. We also fixed $k = 1$ to generate 2-sparse eigenvector cuts as they yielded the best improvement in solving time. Table I compares the computation time of the MILP formulation in [7] with the tightened MILP formulation discussed in this paper. On average, the run time required to find the optimal solution to the tightened MILP decreased by “61%”, which is a non-trivial improvement in comparison to state-of-the-art methods.

We next considered the radial topology design problem with $\hat{\mathcal{E}}$ composed of all edges in the IEEE 39-bus network. Compared to the MILP formulation presented in [7] that required 8,034 sec. to reach the optimal solution, the tightened MILP formulation improved the computation time by 40%. The time required to find the optimal tree was reduced to 4,760 sec. Similarly, we considered the optimal design of a meshed network with 39 edges, where $\hat{\mathcal{E}}$ was composed of all edges in the 39-bus network. The optimal solution in this

TABLE I
COMPARISON OF COMPUTATION TIMES.

Budget(K)	MILP in [7] (sec.)	Tightened MILP (sec.)
5	362	149
6	545	208
7	837	301
8	936	385

case was found in 9 hours. Longer run-times for the latter task can be attributed to looser bounds on the entries of X .

VII. CONCLUSIONS

We have presented tight mathematical formulations and numerous valid inequalities that can substantially speed up the computational time required to find an optimal topology design to enhance stability in power grids. Moreover, we show that our approach, which was previously restricted to the design of radial networks, can be readily extended to the design of meshed grids.

REFERENCES

- [1] E. Tegling, B. Bamieh, and D. F. Gayme, “The price of synchrony: Evaluating the resistive losses in synchronizing power networks,” *IEEE Trans. Control of Network Systems*, vol. 2, no. 3, pp. 254–266, 2015.
- [2] A. Ulbig, T. S. Borsche, and G. Andersson, “Impact of low rotational inertia on power system stability and operation,” *IFAC Proceedings Volumes*, vol. 47, no. 3, pp. 7290–7297, 2014.
- [3] L. Guo, C. Zhao, and S. H. Low, “Graph laplacian spectrum and primary frequency regulation,” in *Proc. IEEE Conf. on Decision and Control*, Miami Beach, FL, Dec. 2018.
- [4] E. Mallada and A. Tang, “Improving damping of power networks: Power scheduling and impedance adaptation,” in *Proc. IEEE Conf. on Decision and Control*, Orlando, FL, Dec. 2011.
- [5] M. Fardad, F. Lin, and M. R. Jovanović, “Design of optimal sparse interconnection graphs for synchronization of oscillator networks,” *IEEE Trans. Autom. Contr.*, vol. 59, no. 9, pp. 2457–2462, 2014.
- [6] D. Deka, H. Nagarajan, and S. Backhaus, “Optimal topology design for disturbance minimization in power grids,” in *Proc. IEEE American Control Conf.*, Seattle, WA, May 2017.
- [7] S. Bhela, D. Deka, H. Nagarajan, and V. Kekatos, “Designing power grid topologies for minimizing network disturbances: An exact MILP formulation,” in *Proc. IEEE American Control Conf.*, Philadelphia, PA, Jul. 2019.
- [8] P. Kundur, *Power system stability and control*. New York, NY: McGraw-Hill, 1994.
- [9] B. K. Poolla, S. Bolognani, and F. Dörfler, “Optimal placement of virtual inertia in power grids,” *IEEE Trans. Autom. Contr.*, vol. 62, no. 12, pp. 6209–6220, Dec. 2017.
- [10] E. Tegling, M. Andreasson, J. W. Simpson-Porco, and H. Sandberg, “Improving performance of droop-controlled microgrids through distributed pi-control,” in *Proc. IEEE American Control Conf.*, Boston, MA, Jul. 2016.
- [11] S. P. Boyd and C. Barratt, *Linear Controller Design: Limits of Performance*. Upper Saddle River, NJ: Prentice-Hall, 1991.
- [12] G. P. McCormick, “Computability of global solutions to factorable nonconvex programs: Part I- convex underestimating problems,” *Mathematical programming*, vol. 10, no. 1, pp. 147–175, 1976.
- [13] H. Nagarajan, M. Lu, E. Yamangil, and R. Bent, “Tightening McCormick relaxations for nonlinear programs via dynamic multivariate partitioning,” in *International Conference on Principles and Practice of Constraint Programming*, Toulouse, France, Sep. 2016.
- [14] S. Boyd and L. Vandenberghe, *Convex Optimization*. New York, NY: Cambridge University Press, 2004.
- [15] W. Ellens, F. Spielsma, P. V. Mieghem, A. Jamakovic, and R. Kooij, “Effective graph resistance,” *Linear Algebra and its Applications*, vol. 435, no. 10, pp. 2491 – 2506, Nov. 2011.
- [16] R. W. Floyd, “Algorithm 97: Shortest path,” *Commun. ACM*, vol. 5, no. 6, p. 345, Jun. 1962.

- [17] C. R. Johnson, “Inverse M-matrices,” *Linear Algebra and its Applications*, vol. 47, pp. 195 – 216, Oct. 1982.
- [18] G. L. Nemhauser, L. A. Wolsey, and M. L. Fisher, “An analysis of approximations for maximizing submodular set functions—I,” *Mathematical Programming*, vol. 14, no. 1, pp. 265–294, 1978.
- [19] I. Dunning, J. Huchette, and M. Lubin, “JuMP: A modeling language for mathematical optimization,” *SIAM Review*, vol. 59, no. 2, pp. 295–320, 2017.
- [20] A. Pai, *Energy function analysis for power system stability*. New York, NY: Springer Science & Business Media, 2012.